Wide temperature range high-speed VCSEL interconnects using FEC and pre-emphasis

Research Article Vol. 33, No. 20 / 6 Oct 2025 / Optics Express 42092
Optics EXPRESS

Wide temperature range high-speed VCSEL interconnects using FEC and pre-emphasis

M. Bilal Aziz,[1,2] Hans Daniel Kaimre,[1,3] and Peter Andrekson[1,4]

[1] *Photonics Laboratory, Department of Microtechnology and Nanoscience, Chalmers University of Technology, Gothenburg 412 58, Sweden*
[2] *bilalaz@chalmers.se*
[3] *kaimre@chalmers.se*
[4] *peter.andrekson@chalmers.se*

Abstract: We present PAM-2 and PAM-4 modulated high-speed 850 nm vertical-cavity surface-emitting laser (VCSEL) based interconnects operating across the temperature range −60°C to 140°C. Two different multiple quantum well VCSEL designs were used along with forward error correction, electronic pre-emphasis, and receiver-side equalization techniques. A three-tap feed-forward equalizer was implemented as a pre-emphasis filter, and a least-mean-square equalizer was used at the receiver. We demonstrate successful PAM-4 transmission at 70 Gb/s from −60°C to 100°C, 50 Gb/s at 125°C, and 42 Gb/s at 140°C. The FEC overhead used in the experiments is 3.1%.

1. Introduction

The rapid advancement of technology and artificial intelligence has greatly increased the demand for high-speed, low-cost, and energy-efficient data centers. To achieve high-speed performance, processor productivity must be improved. Communication between processors and peripheral devices should also match these high speeds while consuming minimal power. Therefore, the role of interconnects and their energy consumption is critical. With increasing data demands, traditional electrical interconnects are becoming inadequate. Optical interconnects have replaced electrical connections because they offer higher bandwidth, lower power consumption, and reduced costs. High-speed, short-reach optical interconnects now play an essential role in enhancing the performance of data centers.

For short-reach optical interconnects up to 100 meters, an 850 nm vertical-cavity surface-emitting laser (VCSEL) combined with multimode fiber (MMF) is normally preferred and is energy efficient as well [1].

To achieve higher data rates within a given system bandwidth, four-level pulse amplitude modulation (PAM4) is preferred over traditional on-off keying (OOK). PAM4 doubles the data rate compared to OOK, making it well-suited for wired networking standards such as Peripheral Component Interconnect Express (PCIe) and Ethernet. However, PAM4 faces greater challenges in maintaining signal integrity. Noise, jitter, and crosstalk from neighboring channels have a more significant impact on PAM4 signals compared to OOK [2].

As the demand for data transfer continues to rise, optical transceivers are placed increasingly closer to heat-generating integrated circuits (ICs) on the circuit board. Currently, the maximum operating temperature for typical datacom module applications is 70∘C. However, automotive, industrial, and sensing applications often require reliable device performance at temperatures above 100∘C. Therefore, optical links must operate efficiently and reliably at higher ambient temperatures [3,4].

Considering the temperature requirements mentioned above, numerous studies have investigated VCSEL-based optical links at elevated temperatures. In 2001, optical links demonstrated on-off

#573616 https://doi.org/10.1364/OE.573616
Journal © 2025 Received 21 Jul 2025; revised 7 Aug 2025; accepted 19 Aug 2025; published 24 Sep 2025

Optics EXPRESS

keying (OOK) transmission rates of 10 Gb/s at 150∘C and 12.5 Gb/s at 140∘C [5]. In 2011, researchers achieved 28 Gb/s OOK transmission at 85∘C [6]. In 2012, data transmission at 14 Gb/s was demonstrated at an elevated temperature of 95∘C [7]. By 2013, OOK transmission reached 40 Gb/s at 85∘C [8], and in 2015, this rate increased further to 50 Gb/s at 90∘C [9]. In 2018, quantum dot VCSELs enabled OOK transmissions of 25 Gb/s at 150∘C, 40 Gb/s at 125∘C, and 45 Gb/s at 105∘C [10]. In 2020, quantum dot VCSELs demonstrated OOK transmission at 25 Gb/s at 180∘C [11]. More recently, in 2021, 25 Gbaud PAM4 signals with clearly open eyes were successfully demonstrated at 125 ∘C [12]. In 2024, 35 Gbaud PAM4 transmission was achieved at room temperature (RT) [13]. That same year, 26.5625 Gbaud PAM4 transmission at 75∘C using 850 nm VCSELs was reported in [14]. In 2025, a 53.125 Gb/s PAM4 transmission at temperatures up to 75∘C was demonstrated using 940 nm VCSELs [15].

In this paper, we present experimental results for PAM2 and PAM4 modulation formats using pre-emphasis, forward error correction (FEC), and equalization across a wide temperature range (−60∘C to 140∘C). To the best of our knowledge, this is the first reported demonstration of VCSEL-based optical interconnects operating at such temperatures.

2. Experimental setup

The experimental setup is shown in Fig. 1. PAM4 and NRZ sequences were generated using a Keysight M8194A Arbitrary Waveform Generator (AWG), which has a maximum sampling rate of 120 GSa/s. A $2^7 - 1$ sequence was used in all experiments to avoid penalties associated with longer sequences. Amplifiers with a bandwidth of 55 GHz were used only for NRZ signal generation to amplify the OOK signals. The AWG output voltage and amplifier gain were adjusted together to achieve optimal peak-to-peak amplitudes for the signals.

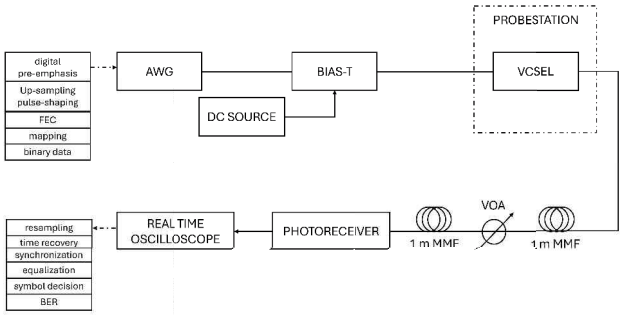

Fig. 1. Experimental setup used for transmissions.

For both NRZ and PAM4 formats, signal pre-emphasis was implemented digitally within the AWG. Pre-emphasis was applied using a finite impulse response (FIR) filter at the transmitter end, resulting in pre-emphasized NRZ and PAM4 signals from the AWG.

The VCSELs presented are detailed in [16] and have an active region with five strained InGaAs/Al0.37Ga0.63As quantum wells (QWs), sandwiched between distributed Bragg reflectors (DBR) comprising of alternating high- and low-index AlGaAs layers, with 2 + 4 oxide layers in the top p-doped DBR. The resonance wavelength of the VCSELs shifts from 843 nm at −60∘C to 856 nm at 140∘C. This study compares two VCSEL designs, one with equal QWs and other with unequal QWs in the active region, also described in detail in [16]. At RT, the pre-emphasized PAM4 signal was fed to the VCSEL at a peak-to-peak amplitude of 0.65 V, whereas the pre-emphasized NRZ signal had a peak-to-peak amplitude of 0.9 V. As temperature increased, the peak-to-peak voltages for both signals were reduced.

Optics EXPRESS

Both VCSELs had an oxide aperture diameter of ≈ 7 microns. The bias current, peak-to-peak voltage, horizontal and vertical eye openings for each VCSEL were optimized at every measurement point in the bit error rate (BER) plot.

The signal was fed into the VCSEL via a Picoprobe RF probe with a bandwidth of 67 GHz. The VCSEL was placed in a moisture-free and light-tight MPI TS200-SE probestation that allows to vary the temperature from −60∘C to 300∘C. The optical output from the VCSEL was coupled into a 1-meter graded-index multimode fiber with a lensed OM4 tip. After the fiber, the signal passed through a variable optical attenuator (VOA) before being received by a MACOM PT 28-F photoreceiver with a 3 dB bandwidth of 32 GHz and a 6 dB bandwidth at 37 GHz. Finally, the electrical output from the photoreceiver was sampled using a Tektronix DPO73304SX real-time oscilloscope with a 33 GHz analog bandwidth and a 100 GSa/s sampling rate (with two active channels). The sampled data was then equalized offline.

3. Measurement results and discussion

3.1. Static and small signal measurements

Figure 2 illustrates the dynamic behavior of the two VCSEL designs across a wide temperature range, based on S21 measurements conducted using a 67 GHz vector network analyzer (VNA - Rohde & Schwarz ZVA67). The complete measurement setup includes RF cables, an RF probe, and a photoreceiver. The response of these components are compensated to isolate the S21 response of the VCSELs.

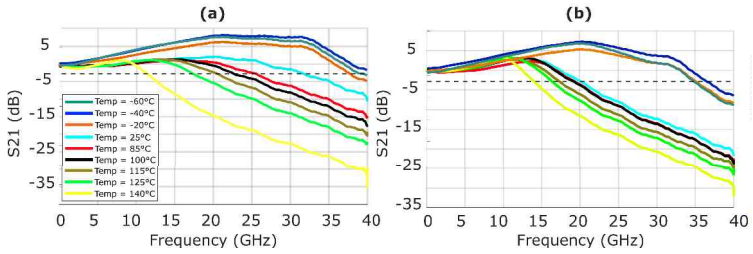

Fig. 2. S21 response of (a) equal QW and (b) unequal QW VCSEL design across temperatures. At sub-zero temperatures, reduction in self-heating allows higher bias currents without thermal rollover, enabling higher modulation bandwidths and output power.

Figure 2(a) shows the VCSEL with equal QWs, while Fig. 2(b) shows the design with unequal QWs. For both designs, the bias currents determined by the optimization algorithm were used for each specific temperature. The optimized bias values were: 17.8 mA at −60°C, 18.6 mA at −40°C, 17.0 mA at −20°C, 15.5 mA at 25°C, 13.6 mA at 50°C, 12.5 mA at 75°C, 10.2 mA at 100°C, 8.5 mA at 125°C, and 7.7 mA at 140°C. At sub-zero temperatures, higher optimized bias currents are feasible due to improved carrier confinement, reduced non-radiative recombination, and enhanced differential gain, which extend the VCSEL's IP curve and enable greater output power without thermal rollover [17–19]. Similar values were fine-tuned and applied for the VCSEL with unequal QWs.

The bias current was not fixed during these measurements. Instead, it was optimized for each temperature to ensure accurate characterization. An optimization algorithm was used to sweep the full range of bias currents and peak-to-peak RF signal voltages $RF_{V_{pp}}$, with BER as the performance metric. The algorithm identified the combination of bias current and $RF_{V_{pp}}$ that yielded the lowest BER, selecting it as the optimal point for each temperature. The process iterated until the global minimum BER was found. This approach was necessary due to the

Optics EXPRESS

significant variation in the current-power (I–P) curves of the VCSELs, especially the shifting of thresholds, saturation points, and the changing slope of the curve with temperature.

At RT (25∘C), the equal QW VCSEL exhibits a 3 dB bandwidth of approximately 32 GHz, compared to 20.3 GHz for the unequal QW VCSEL. As the temperature increases to 75∘C, the bandwidth decreases to 25 GHz for the equal QW and 20 GHz for the unequal QW design. At 140∘C, the 3 dB bandwidth drops further to 11.5 GHz for the equal QW and 14.1 GHz for the unequal QW VCSEL.

A key observation is that the rate of bandwidth degradation with temperature is higher in the equal QW VCSEL. As a result, the unequal QW design maintains better modulation bandwidth at high temperatures and outperforms the equal QW VCSEL under these conditions. In contrast, as the temperature decreases, both designs show improved bandwidth. At -60∘C, the 3 dB bandwidth increases to 39 GHz for the equal QW and 35 GHz for the unequal QW VCSEL.

The reduction in bandwidth and resonance frequency at elevated temperatures is primarily due to reduction of gain and the increasing gain-to-cavity mismatch, also known as detuning. Gain decreases with temperature due to several factors. As temperature increases, the Fermi occupation probability distribution spreads carriers over a larger energy range for a given carrier concentration, thus reducing the concentration of inverted carriers, which in turn causes the gain spectrum to broaden and flatten. In addition, at higher temperatures, non-radiative recombination mechanisms like Auger and defect-related processes become more prominent, reducing the carriers available for radiative recombination and thus decreasing the gain [20]. Wavelength detuning, caused by the mismatch of the gain spectrum and cavity resonance, only augments these effects [21]. Additionally, optical absorption within the distributed Bragg reflectors (DBRs) also increases with temperature [22–24].

To better illustrate these effects, Fig. 3 shows the 3 dB bandwidth of both VCSEL designs throughout the full temperature range. At RT, the equal QW design outperforms the unequal QW design. However, this performance gap narrows as the temperature moves away from the RT, either higher or lower. At extreme high temperatures (e.g. 140∘C), the 3 dB bandwidth of the equal QW VCSEL falls below that of the unequal QW design.

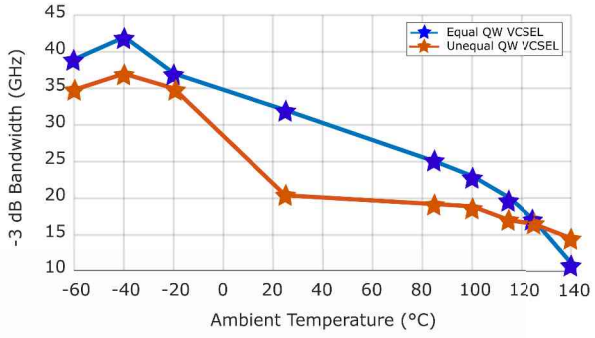

Fig. 3. 3 dB bandwidth of the 2 VCSEL designs versus temperature.

3.2. Large signal measurement

3.2.1. Without pre-emphasis and FEC

Figure 4 shows the back-to-back (BTB) 30 Gbaud BER measurements using the PAM4 modulation scheme across a wide temperature range. An iterative optimization algorithm was employed to determine the optimum bias current and signal voltage for each condition. At the receiver end, a

Optics EXPRESS

real-time oscilloscope with 33 GHz analog bandwidth and 100 GSa/s sampling rate was used to capture the signal after transmission through the link.

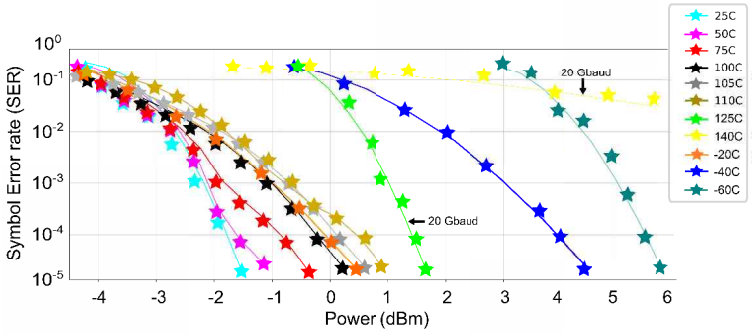

Fig. 4. 30 Gbaud PAM4 BER results without pre-emphasis and FEC using equal QW VCSEL design.

To calculate the BER, a Python-based algorithm was used to identify the optimum sampling point. The algorithm performed a sweep across all possible samples per symbol and calculated the corresponding BER values. It then selected the sample point that for the most times produced the lowest BER. A similar approach was adopted to determine the three optimal vertical threshold levels for the three PAM4 eye openings. The algorithm used nested loops to identify the best threshold values for separating the signal levels, thereby minimizing BER across all three PAM4 eye diagrams.

In the first part of the study, BER measurements were performed without applying any pre-emphasis, forward error correction (FEC), or equalization across different temperatures. These measurements were conducted using the equal quantum well (QW) VCSEL design. The lowest measured BER was below 10^{-4}.

At RT (25∘C), 30 Gbaud PAM4 transmission was achieved at a received power of –1.4 dBm. As the temperature increased to 75∘C, successful transmission required a higher received power of –0.4 dBm. Up to 110∘C, 30 Gbaud PAM4 transmission was still possible, with a received power of 0.9 dBm. This performance exceeds the results reported in [25], where BTB eye diagrams of 30 Gbaud PAM4 transmission were demonstrated only up to 105∘C.

Beyond 110∘C, the reduction in VCSEL modulation bandwidth made 30 Gbaud PAM4 transmission infeasible without pre-emphasis or equalization. As a result, the data rate was reduced to 20 Gbaud for measurements at 125∘C and 140∘C. At 125∘C, PAM4 transmission was achieved with a received power of 1.8 dBm. However, at 140∘C, a severe error floor around 10^{-1} was observed.

In contrast, at lower temperatures, the VCSEL offered sufficient modulation bandwidth to support higher-speed transmission. At –20∘C, 30 Gbaud PAM4 transmission was demonstrated with a received power of 0.4 dBm. The highest system modulation bandwidth was observed at –40∘C, where PAM4 transmission was achieved with a received power of 4.1 dBm. Further reduction in temperature to –60∘C, the lowest reported temperature for PAM4 VCSEL transmission to our knowledge, required a received power of 6.0 dBm for successful operation.

At low temperatures, devices exhibit higher output power at elevated bias currents. This improvement is attributed to enhanced carrier confinement, reduced non-radiative recombination losses, and increased differential gain [26,27].

Optics EXPRESS

3.2.2. With pre-emphasis

Pre-emphasis of the transmitted signal is a powerful technique used to extend the bandwidth of the system. However, it also affects the modulation amplitude. This technique involves applying a filter that adds delayed, weighted versions of the input signal to itself, thereby pre-distorting the transmitted waveform. The pre-distortion compensates for frequency-dependent losses and distortions introduced by the transmission channel [28–32]. In this study, pre-emphasis enabled BTB transmission of PAM4 signals at 125∘C was demonstrated without using forward error correction (FEC) or equalization.

Figure 5 shows the BER performance for different pre-emphasis filter tap configurations at RT and 125C. A baud rate of 30 Gbaud was used for the BER measurements, with 0, 2, 3, 4, and 5 filter taps at RT. However, at 125∘C, due to the presence of severe error floors at 30 Gbaud, the baud rate was reduced to 25 Gbaud. The lowest measured BER across all configurations was below 10^{-4}.

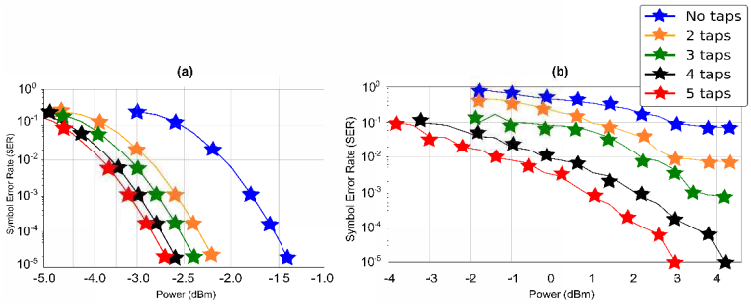

Fig. 5. BER of PAM4 transmission using the equal QW VCSEL design at (a) 30 Gbaud at 25∘C and (b) 25 Gbaud at 125∘C with 0, 2, 3, 4, and 5-tap pre-emphasis filters.

Pre-emphasis was implemented using an iterative algorithm. The algorithm began by capturing a typical received signal and applying a feed-forward equalizer (FFE) at the receiver. A portion of the transmitted sequence (pilot) was used as a reference to estimate the optimized tap coefficients. These coefficients were then applied in a finite impulse response (FIR) filter at the transmitter to generate a pre-emphasized signal, which was transmitted through the link.

At the receiver, the equalizer reprocessed the received signal using the new tap settings and recalculated the BER. If the BER improved, the updated tap coefficients were sent back to the transmitter and reapplied to the FIR filter. This loop continued iteratively until the change in BER became negligible. A learning rate of 10^{-6} was used for the equalizer, which was employed to optimize the equalizer coefficients. A small learning rate led to a higher number of iterations but more accurate convergence to the optimal tap weights for the FIR filter at the transmitter.

Cable calibration was performed prior to the pre-emphasis optimization process, using Keysight IQ tools to ensure accurate signal characterization.

Figure 5(a),(b) illustrates the effects of pre-emphasis at 25∘C and 125∘C, respectively. At RT, transmission without any pre-emphasis taps was demonstrated at a received power of –1.4 dBm. By applying a 2-tap pre-emphasis filter, the received power improved by 0.8 dBm to –2.2 dBm. With 5 taps, further improvement was observed, achieving successful transmission at −2.7 dBm.

At 125∘C, the system showed a severe error floor around 10^{-1}. As the number of taps increased to 3, the error floor dropped below 10^{-3}. With 4 taps, the BER further improved to below 10^{-4}. Finally, with 5 taps, the received power required for transmission improved by 1.1 dBm, enabling transmission at 3 dBm.

These results demonstrate that the impact of pre-emphasis becomes increasingly significant with rising temperature, particularly at 125∘C.

Optics EXPRESS

3.2.3. With FEC

To reduce errors arising primarily from bandwidth limitations and noise, and to improve the BER in our setup, forward error correction (FEC) is required. With FEC, the acceptable BER at the receiver increases, enabling reliable communication at higher error rates. However, FEC introduces overhead, which reduces the effective bit rate of the system. Thus, a trade-off exists between the error correction capability of the FEC and the system's net data rate. FEC also reduces the required signal power for correct detection at the receiver, which in turn allows for lower transmission power. This reduction in power enhances the energy efficiency of both the VCSEL and its driver. Nonetheless, FEC itself consumes energy for encoding and decoding operations [33], so the energy benefits must be balanced with its computational cost.

Historically, the IEEE 802.3 standards have used Reed–Solomon (RS) coding, due to its strong capability to correct burst and symbol errors. However, in short-reach communication systems, this burst-error correction capability is often unnecessary. Instead, FEC schemes designed to correct random bit errors are more suitable.

As data rates continue to increase, hardware limitations and latency have become significant concerns. Consequently, a more efficient FEC tailored for high-speed, short-range applications is needed. Bose–Chaudhuri–Hocquenghem (BCH) codes have emerged as a strong candidate to replace RS codes, offering simpler implementation and lower latency. Specifically, binary BCH codes can be decoded using non-iterative algebraic methods, which further reduces system latency.

Energy consumption is another critical factor in optical link design, affecting both operational costs and environmental impact. Due to their simplicity, BCH codes help reduce system power consumption. In particular, BCH codes with a single-bit error correction capability ($t = 1$) are preferred, where the code length n ranges from 31 to 2047 bits. These codes are denoted as (n, k, t), where k represents the number of information bits. The coding overhead can be computed as the ratio k/n [30,34–36].

PAM4 transmission was used to carry out the measurements. The BCH code length was selected by comparing the performance of various code lengths across the temperature range, including n = 8191, 4095, 1023, 255, and 63. At higher temperatures, stronger error correction is required due to increased signal degradation. However, this must be balanced against the reduction in effective bit rate introduced by FEC overhead. Among the tested options, the BCH(255,247,1) code was found to be the most suitable for short-reach optical links operating across a wide temperature range. This code offers single-bit error correction with a relatively low overhead. The overhead, calculated as $1 - k/n$, is 3.1%. For a 20 Gbaud PAM4 transmission, the resulting net data rate is 19.38 Gbaud, which corresponds to 38.76 Gb/s.

Figure 6 presents the BER curves measured before and after applying BCH FEC at RT and 125 ∘C. The lowest recorded BER was below 10^{-5}. At RT, a modest improvement of 0.4 dBm in received power was observed after applying FEC. At 125 ∘C, the improvement was more significant. Before FEC, successful transmission required a received power of 1.95 dBm. After applying FEC, the required power was reduced to –1.9 dBm, representing an improvement of approximately 4 dBm.

These results demonstrate that the effectiveness of FEC becomes more pronounced at higher temperatures. As thermal effects degrade the signal quality, FEC plays an increasingly critical role in maintaining reliable data transmission.

3.2.4. With pre-emphasis, FEC and receiver equalization

To address challenges such as high-speed operation, low latency, bandwidth limitations, and inter-symbol interference (ISI) in short-reach VCSEL interconnects, techniques such as pre-emphasis, forward error correction (FEC), and receiver-side equalization are employed. The first two techniques have been discussed in previous sections.

Optics EXPRESS

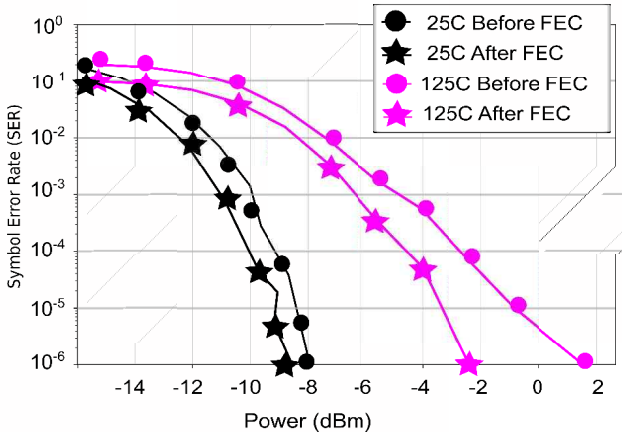

Fig. 6. Experimental BER of a 20 Gbaud PAM4 transmission using BCH(255,247,1) FEC with the equal QW VCSEL design.

A summary of the impact of FEC and pre-emphasis is presented in Fig. 7, based on a 20 Gbaud PAM4 transmission using the equal QW VCSEL design. The data was collected at a BER of 10^{-3}. At RT, the improvement in receiver sensitivity was modest: FEC improved the sensitivity by approximately 0.3 dB, while pre-emphasis provided an improvement of approximately 0.5 dB. As the temperature increased, the benefits of both techniques became more pronounced. At 125 ∘C, FEC enhanced the receiver sensitivity by approximately 2.0 dB, whereas pre-emphasis achieved an improvement of approximately 2.5 dB. Across all measured temperature points, pre-emphasis performed better in improving the receiver sensitivity as compared to FEC. In this section, we introduce receiver equalization in combination with pre-emphasis and FEC to further enhance signal transmission performance across varying thermal conditions.

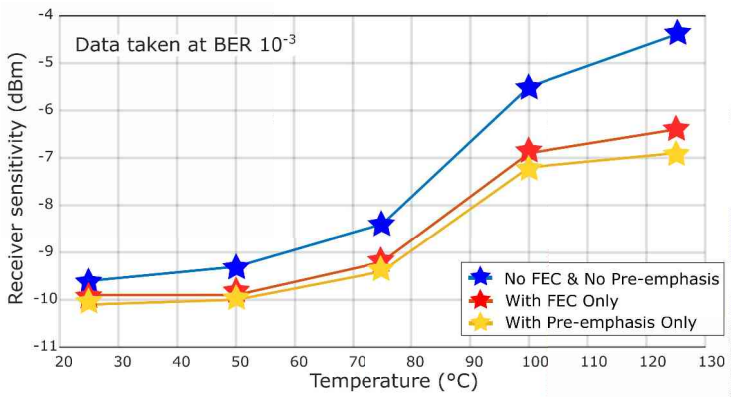

Fig. 7. 20 Gbaud PAM4 transmission showing the effects of FEC and pre-emphasis across temperatures using the equal QW VCSEL design.

Equalization compensates for channel-induced distortions that affect the signal during propagation. In this study, post-processing was performed using an offline least-mean-square (LMS) equalizer. LMS equalization is a widely used adaptive technique in short-reach optical communication systems. Its simplicity and efficiency make it suitable for such links, where the channel typically remains in a relatively stable state during operation.

Optics EXPRESS

Moreover, LMS equalization is capable of adapting to dynamic channel conditions, which is particularly important for optical links where temperature fluctuations can impact VCSEL performance. This adaptability, combined with low computational complexity, makes LMS an effective solution for enhancing signal integrity in thermally variable environments [37–39].

Both PAM4 and PAM2 transmissions were measured and compared using the two VCSEL designs (i.e., equal and unequal quantum wells) across the full temperature range. A 35 Gbaud PAM4 transmission, corresponding to 70 Gb/s (with a net baud rate of 33.915 Gbaud), was demonstrated over the entire temperature range. However, a steep roll-off in the photoreceiver response limited the system's ability to support baud rates beyond 35 Gbaud at RT.

In comparison, PAM2 transmission at 40 Gb/s (with a net bit rate of 38.76 Gb/s) was also demonstrated successfully across the temperature range. These measurements provide a direct comparison of PAM4 and PAM2 performance under thermal stress using both VCSEL designs.

Figure 8 compares PAM2 and PAM4 transmissions using two VCSEL designs: equal QW and unequal QW. Figure 8(a) and Fig. 8(b) correspond to PAM2 using equal and unequal QW VCSELs, respectively, while Fig. 8(c) and Fig. 8(d) represent PAM4 for the same designs. Across all measurements, the BER remained below 10^{-4}.

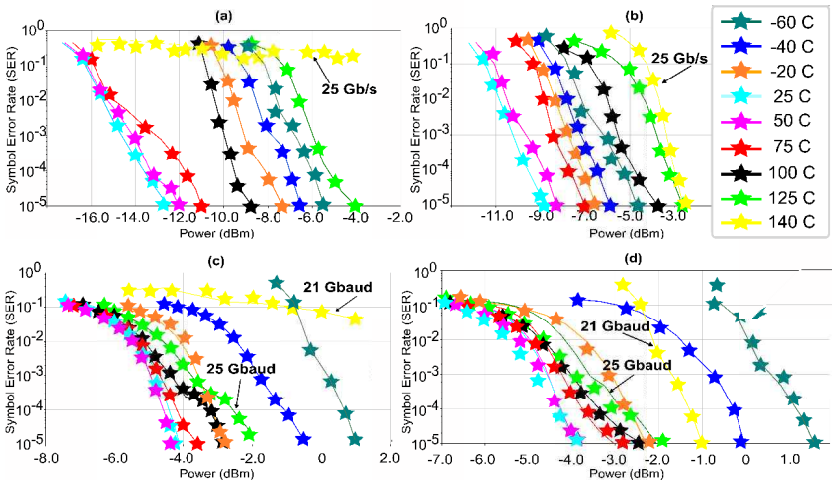

Fig. 8. Experimental (a-b) 40 Gbaud PAM2 and (c-d) 35 Gbaud PAM4 BER results with pre-emphasis, FEC and receiver equalization across wide temperatures using (a,c) equal QW and (b,d) unequal QW VCSEL designs.

For PAM2 transmission at RT, error-free (BER below 10^{-4}) operation was achieved at a received power of –12.9 dBm using the equal QW VCSEL, and –8.9 dBm using the unequal QW VCSEL. At 100∘C, the required received power increased to –9.0 dBm and –3.9 dBm for the equal and unequal QW VCSELs, respectively. By 125∘C, this difference narrowed, with error-free transmission achieved at –4.0 dBm and –2.8 dBm for the equal and unequal QW VCSELs, respectively. At 140∘C, the bitrate was reduced to 25 Gb/s due to bandwidth limitations. Only the unequal QW VCSEL maintained error-free transmission at 2.8 dBm, while the equal QW VCSEL failed to transmit.

At sub-zero temperatures (i.e., –20∘C, –40∘C, and –60∘C), the equal QW VCSEL consistently outperformed the unequal QW VCSEL. The received powers required for error-free PAM2 transmission were –7.2 dBm, –6.8 dBm, and –5.7 dBm for the equal QW VCSEL, and –6.8 dBm, –6.0 dBm, and –4.9 dBm for the unequal QW VCSEL, respectively.

A similar trend was observed for PAM4. The equal QW VCSEL outperformed the unequal design at all temperatures except the extreme case of 140∘C. It can be observed that for error-free

Optics EXPRESS

transmission at RT using PAM4, a significant power penalty is incurred compared to PAM2. Specifically, when using the equal QW VCSEL, the power required for PAM4 transmission was –4.2 dBm, resulting in a power penalty of approximately 8.7 dB relative to PAM2 transmission. For the unequal QW VCSEL, a similar trend is observed. PAM4 transmission at RT was demonstrated at a received power of –3.9 dBm, while PAM2 transmission required 8.9 dBm, corresponding to a power penalty of approximately 5.0 dB. At 100∘C, error-free PAM4 transmission was achieved at –3.0 dBm and –2.5 dBm for the equal and unequal QW VCSELs, respectively. At 125∘C, the baud rate was reduced to 25 Gbaud to maintain transmission, requiring received powers of –2.1 dBm and –1.9 dBm. At 140∘C, the bitrate was further lowered to 21 Gbaud, and only the unequal QW VCSEL achieved error-free transmission at –1.0 dBm. To our knowledge, this is the highest PAM4 transmission bit rate reported at 140∘C for a VCSEL interconnect.

At sub-zero temperatures, 35 Gbaud PAM4 error-free transmission was successfully demonstrated using both VCSEL designs. The required received powers for the equal QW VCSEL were –2.9 dBm, –0.6 dBm, and 0.9 dBm at –20∘C, –40∘C, and –60∘C, respectively. For the unequal QW VCSEL, the corresponding values were –2.2 dBm, –0.1 dBm, and 1.5 dBm. To the best of our knowledge, these results represent the first reported demonstrations of PAM4 VCSEL interconnect transmission at these sub-zero temperatures. The corresponding eye diagrams are presented in Fig. 9. It can be observed that the maximum eye opening occurs at Fig. 9(a), corresponding to –60°C, while the eye is nearly closed in Fig. 9(f), at 140°C. These eye diagrams were captured at the receiver side (prior to receiver equalization).

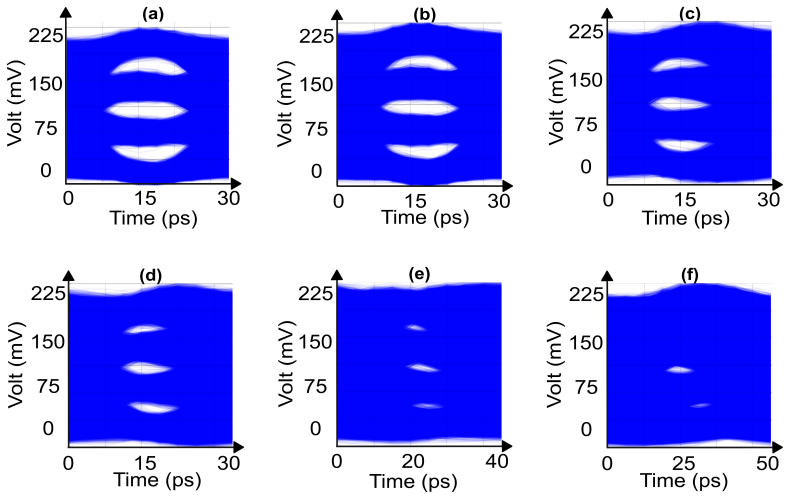

Fig. 9. Experimental PAM4 eye diagrams before receiver equalization, using equal QW VCSELs, at the following conditions: (a) 35 Gbaud at –60°C, (b) 35 Gbaud at –20°C, (c) 35 Gbaud at 25°C, (d) 35 Gbaud at 100°C, (e) 25 Gbaud at 125°C, and (f) 21 Gbaud at 140°C.

4. Conclusion

We have demonstrated high data rate transmission of 70 Gb/s using PAM4 and 40 Gb/s using PAM2 with VCSELs, employing both equal and unequal quantum well (QW) VCSEL designs across a wide temperature range. High temperatures pose unique challenges for VCSEL performance, primarily due to reduced modulation bandwidth caused by increased non-radiative recombination processes. At extreme temperatures, particularly 140∘C, the unequal QW VCSEL design outperforms the equal QW counterpart. Notably, PAM4 data transmission at 42 Gb/s was successfully demonstrated at 140∘C using the unequal QW VCSEL.

Optics EXPRESS

To enhance system performance, techniques such as BCH-based forward error correction (FEC), pre-emphasis, and receiver-side equalization were employed. The sensitivity penalty associated with high temperatures reduces the optical link budget, making it essential to adopt energy-efficient strategies—such as low-overhead BCH-FEC and minimal-tap filters—to maintain sufficient power levels for error-free transmission across all temperatures.

Additionally, this work demonstrates successful data transmission at sub-zero temperatures using both PAM2 and PAM4 modulation formats. The observed increase in modulation bandwidth at lower temperatures provides valuable insight, indicating that deliberate control of ambient temperature can be an effective approach to enhance modulation bandwidth and improve overall system performance.

Funding. Stiftelsen för Strategisk Forskning (CHI19-0004).

Acknowledgment. The authors would like to thank Dr. Stavros Giannakopoulos for his assistance with assisting lab measurements. The authors acknowledge the use of AI systems for grammar enhancement purposes.

Disclosures. The authors declare no conflicts of interest.

Data availability. Data underlying the results presented in this paper are not publicly available at this time but maybe obtained from the authors upon reasonable request.

References

1. Y. Xu, C. Yang, Z. Xu, *et al.*, "Optics-Informed Fully Convolutional Networks for Enhanced Channel Equalization in High-Speed VCSEL-Based Optical Interconnects," in *2024 Asia Communications and Photonics Conference (ACP) and International Conference on Information Photonics and Optical Communications (IPOC)* (IEEE, 2024), pp. 1–4.
2. C. Zhang, F. Chen, L. Wang, *et al.*, "Recent Advances of High-Speed Short-Reach Optical Interconnects for Data Centers," IEEE Open Journal of the Solid-State Circuits Society (2025).
3. M.-G. A. E. S. Group, "IEEE 802.3 Multi-Gigabit Automotive Ethernet Study Group Ad Hoc Area," (2017). Accessed: 2025-12-05.
4. C. Tabbert and C. Kuznia, "Chip scale package fiber optic transceiver integration for harsh environments," in *International Conference on Space Optics—ICSO 2014*, vol. 10563 (SPIE, 2017), pp. 903–908.
5. F. Peters and M. MacDougal, "High-speed high-temperature operation of vertical-cavity surface-emitting lasers," IEEE Photonics Technol. Lett. **13**(7), 645–647 (2001).
6. J.-W. Shi, W.-C. Weng, F.-M. Kuo, *et al.*, "Oxide-relief vertical-cavity surface-emitting lasers with extremely high data-rate/power-dissipation ratios," in *Optical Fiber Communication Conference* (Optica Publishing Group, 2011), p. OThG2.
7. L. A. Graham, H. Chen, D. Gazula, *et al.*, "The next generation of high speed VCSELs at Finisar," in *Vertical-Cavity Surface-Emitting Lasers XVI*, vol. 8276 (SPIE, 2012), pp. 13–22.
8. P. Westbergh, R. Safaisini, E. Haglund, *et al.*, "High-Speed Oxide Confined 850-nm VCSELs Operating Error-Free at 40 Gb/s up to 85C," IEEE Photonics Technol. Lett. **25**(8), 768–771 (2013).
9. D. M. Kuchta, A. V. Rylyakov, C. L. Schow, *et al.*, "A 50 Gb/s NRZ modulated 850 nm VCSEL transmitter operating error free to 90 C," J. Lightwave Technol. **33**(4), 802–810 (2015).
10. N. Ledentsov Jr, M. Agustin, V. A. Shchukin, *et al.*, "Quantum dot 850 nm VCSELs with extreme high temperature stability operating at bit rates up to 25 Gbit/s at 150°C," Solid-State Electron. **155**, 150–158 (2019).
11. N. Ledentsov, L. Chorchos, O. Makarov, *et al.*, "Quantum-dot oxide-confined 850-nm VCSELs with extreme temperature stability operating at 25 Gbit/s up to 180deg C," in *Vertical-Cavity Surface-Emitting Lasers XXIV*, vol. 11300 (SPIE, 2020), pp. 90–96.
12. T. Aoki, R. Kubota, H. Hiiro, *et al.*, "50 Gb/s PAM-4 VCSELs operating up to 125°C," in *2021 Opto-Electronics and Communications Conference (OECC)* (2021), pp. 1–3.
13. A. Liu, B. Tang, Z. Li, *et al.*, "Gbps PAM-4 850-nm oxide-confined VCSEL without equalization and pre-emphasis [J]," Journal of Semiconductors **5**, (70).
14. Y.-C. Yang, W.-H. Chen, C.-C. Chiu, *et al.*, "26.5625 Gbaud PAM-4 short-reach transmission at 75°C using 850 nm VCSELs with strategic oxide guiding layer positioning," Opt. Lett. **49**(8), 2077–2080 (2024).
15. Y.-C. Yang, Z. Wang, C.-C. Chiu, *et al.*, "53.125 Gbps PAM-4 transmission up to 75 C using 940-nm VCSELs on 330 μm Ge substrates for datacom applications," in *Vertical-Cavity Surface-Emitting Lasers XXIX*, vol. 13384 (SPIE, 2025), pp. 21–27.
16. H. D. Kaimre, A. Grabowski, J. Gustavsson, *et al.*, "25 Gbaud 850 nm VCSEL for an Extended Temperature Range," IEEE Photonics Technology Letters (2025).
17. F. Z. Jasim, K. Omar, Z. Hassan, *et al.*, "Temperature effect on VCSEL output performance," J. Optoelectron. Adv. Mater **3**, 1136–1138 (2009).
18. T. E. Sale, J. S. Roberts, J. P. David, *et al.*, "Temperature effects in VCSELs," in *Vertical-Cavity Surface-Emitting Lasers*, vol. 3003 (SPIE, 1997), pp. 100–110.

Optics EXPRESS

19. H. Li, J. A. Lott, P. Wolf, *et al.*, "Temperature-dependent impedance characteristics of temperature-stable high-speed 980-nm VCSELs," IEEE Photonics Technol. Lett. **27**(8), 832–835 (2015).
20. L. A. Coldren, S. W. Corzine, and M. L. Mashanovitch, *Diode lasers and photonic integrated circuits* (John Wiley & Sons, 2012).
21. H. D. Kaimre, A. Grabowski, J. Gustavsson, *et al.*, "Effects of detuning on wide-temperature behavior of 25 Gbaud 850nm VCSELs," in *Vertical-Cavity Surface-Emitting Lasers XXVII*, vol. 12439 (SPIE, 2023), pp. 92–104.
22. R. N. Hall, "Electron-hole recombination in germanium," Phys. Rev. **87**(2), 387 (1952).
23. W. Shockley and W. Read Jr, "Statistics of the recombinations of holes and electrons," Phys. Rev. **87**(5), 835–842 (1952).
24. H. Kaimre, "Vertical-Cavity Surface-Emitting Lasers with Improved Wide-Temperature Dependence," Licentiate Thesis (2025).
25. Y.-C. Yang, H.-T. Cheng, T.-H. Liu, *et al.*, "Volume manufacturable oxide-confined 850-nm VCSELs operating at 25-50 Gbps up to 105°C without equalization and pre-emphasis," in *Vertical-Cavity Surface-Emitting Lasers XXVI*, vol. 12020 (SPIE, 2022), pp. 65–72.
26. D. Wu, W. Fu, H. Wu, *et al.*, "Cryogenic VCSEL microwave-optical model for laser frequency response prediction and e–h recombination lifetime analysis," J. Appl. Phys. **132**(22), 223101 (2022).
27. A. Liu, C. Hao, T. Yu, *et al.*, "High-speed 850 nm oxide-confined vertical-cavity surface-emitting lasers at high temperature and cryogenic temperature," J. Phys. Photonics **7**(3), 035003 (2025).
28. H.-Y. Kao, C.-T. Tsai, S.-F. Leong, *et al.*, "Single-mode VCSEL for pre-emphasis PAM-4 transmission up to 64 Gbit/s over 100–300 m in OM4 MMF," Photonics Res. **6**(7), 666–673 (2018).
29. K. Szczerba, T. Lengyel, Z. He, *et al.*, "High-speed optical interconnects with 850nm VCSELS and advanced modulation formats," in *Vertical-Cavity Surface-Emitting Lasers XXI*, vol. 10122 (SPIE, 2017), pp. 109–116.
30. T. Lengyel, *Multilevel Modulation and Transmission in VCSEL-based Short-range Fiber Optic Links* (Chalmers Tekniska Hogskola (Sweden), 2019).
31. T. Lengyel, E. Simpanen, J. Gustavsson, *et al.*, "Pre-emphasis enabled 50 Gbit/s transmission over 1000 m SMF using a 1060 nm single-mode VCSEL," Electron. Lett. **54**(20), 1186–1187 (2018).
32. J. Chen, Z. S. He, T. Lengyel, *et al.*, "An Energy Efficient 56 Gbps PAM-4 VCSEL Transmitter Enabled by a 100 Gbps Driver in 0.25 μm InP DHBT Technology," J. Lightwave Technol. **34**(21), 4954–4964 (2016).
33. K. Szczerba, C. Fougstedt, P. Larsson-Edefors, *et al.*, "Impact of forward error correction on energy consumption of VCSEL-based transmitters," in *2015 European Conference on Optical Communication (ECOC)* (IEEE, 2015), pp. 1–3.
34. T. Lengyel, K. Szczerba, M. Karlsson, *et al.*, "Demonstration of a 71.8 Gbps 4-PAM 850 nm VCSEL-based link with a pre-emphasizing passive filter," in *ECOC 2016; 42nd European Conference on Optical Communication* (VDE, 2016), pp. 1–3.
35. R. R. Lopez, M. Mueller, B. Li, *et al.*, "High-speed 1550 nm VCSEL data transmission link employing 25 Gbaud 4-PAM modulation and Hard Decision Forward Error Correction," J. Lightwave Technol. **31**(4), 689–695 (2013).
36. T. Wettlin, Y. Lin, N. Stojanovic, *et al.*, "200Gb/s VCSEL transmission using 60m OM4 MMF and KP4 FEC for AI computing clusters," arXiv (2024).
37. K. Szczerba, T. Lengyel, M. Karlsson, *et al.*, "94-Gb/s 4-PAM using an 850-nm VCSEL, pre-emphasis, and receiver equalization," IEEE Photonics Technol. Lett. **28**(22), 2519–2521 (2016).
38. G. Belfiore, R. Henker, and F. Ellinger, "The effect of strong equalization in high-speed VCSEL-based optical communications up to 48 Gbit/s," in *2016 IEEE Bipolar/BiCMOS Circuits and Technology Meeting (BCTM)* (IEEE, 2016), pp. 13–16.
39. M. Srinivasan, J. Song, A. Grabowski, *et al.*, "End-to-end learning for VCSEL-based optical interconnects: state-of-the-art, challenges, and opportunities," J. Lightwave Technol. **41**(11), 3261–3277 (2023).